Sources, pathways and drivers of Sub-Antarctic Mode Water formation

Bieito Fernández Castro[1], Alberto C. Naveira Garabato[1], Matthew Mazloff[2]and Richard G. Williams[3].

[1]Ocean and Earth Science, National Oceanography Centre, University of Southampton, Southampton, UK
[2]Scripps Institution of Oceanography, University of California, San Diego, La Jolla, CA, USA
[3]Department of Earth, Ocean, and Ecological Sciences, School of Environmental Sciences, University of Liverpool, UK

Key Points:

- Sub-Antarctic Mode Waters originate from both southward-flowing subtropical thermocline waters and northward-flowing Circumpolar Deep Water
- Sub-Antarctic Mode Water formation is dominated by subtropical sources in the Indian Ocean versus Antarctic sources in the Pacific Ocean
- Northern and southern sources undergo contrasting surface heat and freshwater fluxes and interior mixing to become Sub-Antarctic Mode Waters

Corresponding author: Bieito Fernández Castro, b.fernandez-castro@soton.ac.uk

Abstract

Sub-Antarctic Mode Waters (SAMWs) form to the north of the Antarctic Circumpolar Current (ACC) in the Indo-Pacific Ocean, whence they ventilate the ocean's lower pycnocline and play an important role in the climate system. With a backward Lagrangian particle-tracking experiment in a data-assimilative model of the Southern Ocean (B-SOSE), we address the long-standing question of the extent to which SAMWs originate from densification of southward-flowing subtropical waters versus lightening of northward-flowing Antarctic waters sourced by Circumpolar Deep Water (CDW) upwelling. Our analysis evidences the co-occurrence of both sources in all SAMW formation areas, and strong inter-basin contrasts in their relative contributions. Subtropical waters are the main precursor of Indian Ocean SAMWs (70-75% of particles) but contribute a smaller amount (<40% of particles) to Pacific SAMWs, which are mainly sourced from the upwelled CDW. By tracking property changes along particle trajectories, we show that SAMW formation from northern and southern sources involves contrasting drivers: subtropical source waters are cooled and densified by surface heat fluxes, and freshened by ocean mixing. Southern source waters are warmed and lightened by surface heat and freshwater fluxes, and they are made either saltier by mixing in the case of Indian SAMWs, or fresher by surface fluxes in the case of Pacific SAMWs. Our results underscore the distinct climatic impact of Indian and Pacific SAMWs formation, involving net release of atmospheric heat and uptake of atmospheric freshwater, respectively; a role that is conferred by the relative contributions of subtropical and Antarctic sources to their formation.

Plain Language Summary

The formation of Sub-Antarctic Mode Waters (SAMWs) in the sub-Antarctic Zone of the southern Indo-Pacific Ocean is crucial for the transfer of large amounts of heat and carbon dioxide to the ocean interior, thereby mitigating climate change. Despite their importance, there are contrasting views regarding the origins and history of these water masses prior to subduction, which determine the waters' heat and carbon sequestration capacity. Using a state-of-the-art ocean model constrained by observations, we identify and track the sources of SAMWs and quantify their heat exchange with the atmosphere. Our results confirm the co-existence of two sources of SAMWs: warm, shallow subtropical waters and cold, deep Antarctic waters. The formation of SAMW from contrasting sources has distinct impacts on the climate system. On their path to SAMW formation, subtropical waters release heat into the atmosphere, whilst Antarctic waters absorb heat. Furthermore, subtropical and Antarctic sources dominate SAMW formation in the Indian and Pacific Oceans, respectively, highlighting the contrasting nature of the two main pools of SAMW. Our results shed new light on the intricate nature of SAMWs, helping to predict and understand their role in slowing down future climate change.

1 Introduction

Sub-Antarctic Mode Waters (SAMWs) form through convective mixing in a relatively narrow latitudinal band of deep (>300 m) winter mixed layers to the north of the sub-Antarctic front at the equatorward edge of the Antarctic Circumpolar Current (ACC) (Hanawa & Talley, 2001) in the central and eastern Pacific and Indian oceans (Sallée et al., 2010), and go on to ventilate a large fraction of the ocean's pycnocline (Jones et al., 2016). As such, SAMWs are a key component of the Southern Ocean's and global overturning circulation (Speer et al., 2000; Marshall & Speer, 2012; Morrison et al., 2022), and play a crucial climatic role in the sequestration of heat and carbon. Collectively, SAMWs account for more than half of the heat gained by the upper Southern Hemisphere's oceans during 2006–2013 (Roemmich et al., 2015), hold ∼20% of the total ocean anthropogenic carbon inventory (Iudicone et al., 2011; Groeskamp, Lenton, et al., 2016; Gruber et al., 2019), and transport nutrients away from the surface Southern Ocean to fuel carbon export in other ocean basins (Sarmiento et al., 2004; Hauck et al., 2018).

Despite the importance of SAMWs, there remain fundamental knowledge gaps on how SAMWs are formed, hampering our ability to fully appraise their climatic role and their evolution under climate change. Different threads of research have identified two contrasting sources and pathways for the formation of SAMWs, with divergent implications for heat and carbon uptake, and nutrient redistribution. One of the paradigms focuses on the formation of SAMWs from relatively cold, carbon- and nutrient-rich Circumpolar Deep Waters (CDW) (e.g., Speer et al. (2000); Sarmiento et al. (2004); Panassa et al. (2018)). Circumpolar westerly winds induce CDW upwelling south of and around the ACC, and their subsequent northward transport across the sub-Antarctic Front via Ekman dynamics (Marshall & Speer, 2012). Along their path, CDW are lightened by surface and ocean-ice heat and freshwater fluxes, forming SAMWs (Abernathey et al., 2016; Evans et al., 2018; Tamsitt et al., 2018). As old and carbon-rich waters, carbon dioxide is released into the atmosphere when CDW are entrained into the mixed layer along their way to the SAMW formation regions (Chen et al., 2022; Prend et al., 2022).

In the complementary paradigm, SAMWs formation is seen as preferentially fed by relatively warm, nutrient-poor subtropical thermocline waters (McCartney, 1977; Sloyan & Rintoul, 2001; Talley et al., 2003; Iudicone, Madec, et al., 2008; Iudicone et al., 2011). Subtropical waters move southward within western boundary currents, primarily the Agulhas current, eventually joining the northern flank of the ACC (Wang et al., 2014), which advects them eastward towards the different SAMW formation regions. Along their paths, northern ACC waters lose heat to the atmosphere, becoming denser to form SAMWs (McCartney, 1977; Talley et al., 2003; Iudicone, Madec, et al., 2008). Cooling increases gas solubility in these SAMW precursor water-masses, driving a net uptake of atmospheric carbon dioxide (Iudicone et al., 2011; Gray, 2024).

Although these views appear in contrast, there is extensive evidence for the co-existence of Antarctic (originating in CDW upwelling) and subtropical contributions to SAMW formation in the observational and modelling literature. Inverse model analysis of hydrographic sections (Sloyan & Rintoul, 2001), as well as Lagrangian and water-mass transformation diagnoses of model data (Iudicone, Speich, et al., 2008; Iudicone et al., 2011; Cerovečki & Mazloff, 2016) evidence that SAMW formation is fed by both upwelling and subsequent lightening of CDW, as well as densification of subtropical thermocline waters. Furthermore, recent research has highlighted the influence of Antarctic sources on the interannual variability of SAMW freshwater content and mixed layer depths in the Pacific Ocean (Rintoul & England, 2002; Meijers et al., 2019; Cerovečki et al., 2019), whilst the remote influence of western boundary currents – linking SAMW with the subtropics – is apparent in adjoint model experiments (Boland et al., 2021). The subtropical influence is also noticeable in biogeochemical Argo observations (Fernández Castro et al., 2022), revealing a seasonal increase of salinity and decrease of nutrient concentrations

within the summer thermocline of SAMW formation regions, which was attributed to the advection of subtropical waters along the ACC.

A notable feature of SAMWs is the existence of several pools in the Indo-Pacific ocean, stemming from different regions of formation in deep winter mixed layers (Sallée et al., 2010; Herraiz-Borreguero & Rintoul, 2011; Bushinsky & Cerovečki, 2023). The temperature and salinity values characterising the different SAMW pools decrease eastward from the western Indian to the eastern Pacific oceans, while the nutrient content increases (McCartney, 1977; Sallée et al., 2010; Herraiz-Borreguero & Rintoul, 2011; Bushinsky & Cerovečki, 2023). These large-scale property patterns may be interpreted as the result of a varying degree of subtropical influence in the different SAMW pools (Fernández Castro et al., 2022; Bushinsky & Cerovečki, 2023) – with the largest subtropical influence in the western Indian Ocean downstream of the ACC's encounter with the warm and salty waters of the Agulhas current (Sloyan & Rintoul, 2001; Wang et al., 2014) – yet this hypothesis has not yet been directly tested.

In this study, we quantify and contrast the role of subtropical and Circumpolar Deep Water sources in the formation of the different pools of SAMW by means of a backward Lagrangian particle tracking experiment using output from a physical-biogeochemical Southern Ocean State Estimate (B-SOSE) (Verdy & Mazloff, 2017). Specifically, we: (1) quantify the relative contributions of subtropical and Antarctic sources to the different SAMW pools in the Indian and Pacific Oceans; (2) quantify the processes (surface fluxes and interior mixing) that transform the precursor water masses into SAMWs, clarifying the role of different pathways as sources or sinks of heat to the atmosphere; (3) map these fluxes onto geographical and property (temperature-salinity) spaces to reveal the sequence of processes leading to SAMW formation from the different sources.

The manuscript is structured as follows. In Section 2, we describe the Lagrangian experiment and subsequent analysis of particle trajectories. In Section 3, we first quantify the contribution of the different sources of SAMWs and characterise them in terms of their origins, pathways and associated time scales (Section 3a). A time scale analysis includes an estimate of the time spent by the particles in the mixed layer (Section 3b). We then quantify water mass transformations (changes in temperature, salinity and density) along trajectories, and identify their underpinning processes by distinguishing between contributions from surface fluxes and interior mixing (Section 3c). Next, we map these transformations onto geographical and property spaces to reveal the sequence of events leading to the formation of SAMWs (Section 3d). Finally, we summarise and discuss our results in Section 4, and outline wider implications in Section 5.

2 Methods

2.1 Model output and particle-tracking experiment

The Lagrangian experiment was conducted with the OceanParcels Python virtual particle tracking toolbox (Lange & van Sebille, 2017; Delandmeter & van Sebille, 2019), using 5-daily output from the Biogeochemical Southern Ocean State Estimate (B-SOSE) (Verdy & Mazloff, 2017; Mazloff et al., 2010) iteration 139, covering from January 2013 to December 2021. B-SOSE is a regional coupled biogeochemical-sea-ice-ocean model with a 1/6° horizontal spatial resolution, forced by optimized atmospheric reanalysis fields from ERA-Interim (Dee et al., 2011). The model assimilates physical and biogeochemical observations, including from biogeochemical profiling floats, to create a coherent picture of Southern Ocean processes that conserves mass and has closed budgets for biogeochemical properties. B-SOSE and its physics-only predecessor, SOSE, have been extensively used in recent years to investigate water mass pathways and physical and biogeochemical processes in the Southern Ocean (Wang et al., 2014; Abernathey et al., 2016; Tamsitt et al., 2016, 2017; Ellison et al., 2023), adequately reproducing the observed prop-

erties, spatial distribution and temporal dynamics of SAMWs (Cerovečki et al., 2013; Cerovečki & Mazloff, 2016). Relevantly, (B-)SOSE has been used to investigate CDW upwelling pathways and their associated water mass transformations (Tamsitt et al., 2017, 2018); however, the fate of the upwelled waters and their transformation into SAMWs has not been explored yet.

For our experiment, 100,000 particles were released in the SAMW formation regions over the 9 years of the original B-SOSE simulation (January 2013 – December 2021). The particles were initialised at random times and depths within the surface mixed layer. The particles were only retained for simulation if the depth of the mixed layer at the seeding time and location exceeded 300 m, otherwise they were discarded. This procedure effectively selects regions of deep winter mixed layers in the northern flank of the ACC, that is, regions of SAMW formation during the winter season (Fig. 1). Since the modelled mixed layer depths are shallower than 300 m everywhere outside the SAMW formation regions, it was not necessary to introduce additional constraints (e.g., geographical) to the particle seeding algorithm.

The particles were tracked backward in time for 25 years or until they left the Southern Ocean, moving northward across 30°S. For this, the model output was looped four times, with a total simulation time of 36 years (to account for the fact that particles are seeded over a time span of 9 years). The integration was performed with a one-hour time step and the particle positions were recorded every 5 days. We chose not to focus on interannual variability and analysed all particles together, irrespective of their release year, in order to obtain a time-mean picture of SAMW formation pathways during the B-SOSE simulation period. To account for the effect of surface-intensified mixing, particles reaching the mixed layer were randomly reshuffled within the mixed layer every 5 days. Sensitivity tests were performed with more frequent reshuffling (once every day and once every hour), to ensure that the specific choice had no impact on the results. Only unrealistically weak mixing (one reshuffling every 20 days), resulted in significantly altered particle pathways.

2.2 Analysis of particle pathways and water mass transformations

The origins and pathways of the particles were studied by assessing their location within the frontal zones of the ACC as a function of the backward time since their release. The frontal zones were computed by applying the definitions of the ACC fronts in Orsi et al. (1995) to the time-mean potential temperature and practical salinity fields; thus, the identified frontal features represent the time-mean locations of the fronts in B-SOSE. The frontal zones, marked in Fig. 1, include from south to north: the Antarctic Zone (AZ), Southern ACC zone (S-ACC), the Polar Frontal Zone (PFZ), the Sub-Antarctic Zone (sub-AZ) and the Subtropical Zone (STZ). The zones are separated, from south to north, by the ACC Southern Boundary (SB), the Polar Front (PF), the Sub-Antarctic Front (sub-AF) and the Subtropical Front (STF). A significant number of particles tended to leave the model domain toward lower latitudes along continental boundaries, mainly through the western boundary currents (WBCs) along South America (Brazil Current), Eastern Australia (East Australian Current) and South Africa (Agulhas Current), but also along western Australia and eastern New Zealand. The number of particles transiting or leaving the model domain along continental boundaries was quantified by defining polygons delineating those systems (see Fig. 1). The relative importance of source waters and pathways for the different SAMW varieties was studied by classifying the particles by their release location within the main SAMW formation regions: central Indian (40–120°E), east Indian (120–190°E), central Pacific (190–250°E), and east Pacific (250–310°E).

To assess the water mass transformations along Lagrangian pathways, water properties (potential temperature and salinity) and surface fluxes (net heat and freshwater

fluxes into the ocean) interpolated at the particles' positions were recorded every five days. From the recorded quantities, conservative temperature (Θ), absolute salinity (S_A) and potential density (σ_Θ) were derived. The contributions of surface fluxes (herewith abbreviated as s-f) to changes (Δ) in Θ and S_A between two consecutive particle observations were estimated based on mixed layer heat and salt budgets, by assuming negligible downward shortwave radiation flux across the mixed layer base and quasi-instantaneous (in less than the output's time-step, i.e. 5 days) homogenization by vertical mixing within the mixed layer:

$$\Delta\Theta^{\text{s-f}} \approx \frac{Q}{h_{ML}\rho C_p}\,\Delta t, \quad |z| \le h_{ML}, \tag{1}$$

$$\Delta\Theta^{\text{s-f}} = 0, \quad |z| > h_{ML}, \tag{2}$$

and

$$\Delta S_A^{\text{s-f}} \approx \frac{S_A\,\text{FWF}}{h_{ML}\rho}\,\Delta t, \quad |z| \le h_{ML}, \tag{3}$$

$$\Delta S_A^{\text{s-f}} = 0, \quad |z| > h_{ML}. \tag{4}$$

Here Q, FWF, h_{ML} and ρ are the surface heat and freshwater fluxes, mixed layer depth and density, respectively, averaged for two consecutive observations; C_p is the heat capacity of seawater; Δt is the time-step of 5 days, and z is the averaged particle depth. Therefore, the contribution of surface fluxes to temperature and salinity transformations is only accounted for when particles are located within the mixed layer. The effect of shortwave radiation depth penetration, which has little impact on the derived transformations in the Southern Ocean (less than 5% of surface radiation penetrates below the mixed layer; Groeskamp and Iudicone (2018); Evans et al. (2018)), is ignored. The contribution of the surface fluxes to σ_Θ changes was estimated as $\sigma_\Theta^{\text{s-f}} = -\alpha\,\Delta\Theta^{\text{s-f}} + \beta\,\Delta S_A^{\text{s-f}}$, where α and β are the thermal expansion and haline contraction coefficients, respectively. The contribution of sub-grid-scale processes (i.e. ocean mixing) to water mass transformations along Lagrangian pathways was then estimated from the residual between the net changes between consecutive observations ($\Delta\Theta^{\text{net}}$, ΔS_A^{net}, and $\Delta\sigma_\Theta^{\text{net}}$) and the surface flux-driven change: $\Delta\Theta^{\text{res}} = \Delta\Theta^{\text{net}} - \Delta\Theta^{\text{s-f}}$, where the same applies to S_A and σ_Θ.

To gain further insight into water mass transformations, we classified particle trajectories leading to the different SAMW formation regions into two main pathways: a northern pathway for particles originating to the north of the sub-Antarctic Front, and a southern pathway for particles originating to the south of the sub-Antarctic Front. Particles are classified as part of the northern pathway if they leave the tracking domain northward across 30°S at some point during the backward-tracking simulation, or if they are located north of the sub-Antarctic Front at the end of the 25 years of tracking. Particles are classified as part of the southern pathway if they are located south of the sub-Antarctic Front at the end of the 25 years of backward tracking. None of the particles in the southern pathway leave the domain, so there is no risk of ambiguity in this classification.

Mean transformations, and contributions from surface fluxes and mixing, were calculated as

$$\overline{\Delta\Theta^{(\text{net, s-f, res})}}_{k,l} = \frac{1}{n_{par}^{k,l}} \sum_{i=1}^{n_{par}^{k,l}} \sum_{j=1}^{n_{obs}^{i}} \left(\Delta\Theta_{i,j}^{(\text{net, s-f, res})}\right) \tag{5}$$

for each pathway (k) and formation region (l). Here $n_{par}^{k,l}$ is the number of particles released in region l that follow pathway k, and n_{obs}^{i} is the total number of 5-daily observations of particle i. The changes and fluxes were also mapped spatially onto a longitude-latitude grid, and as a function of water mass properties onto a $\Theta{-}S_A$ grid. This mapping was done by restricting the summation in Eq. 5 to particles (i) and observations (j) within the specified grid cells, in such a way that the summation over all cells for a region and pathway adds up to the mean property change in Eq. 5.

3 Results

3.1 Particle origins and pathways

The particle tracking experiment revealed a wide range of water mass pathways leading to the formation of SAMWs, which can be essentially separated into southern Antarctic and northern subtropical pathways. These pathways and their general characteristics are succinctly illustrated by two example particles released in the same SAMW formation region in the central Pacific (Fig. 2). The particles initially travelled (backward in time) westward in close mutual proximity across the whole Pacific and part of the Indian Ocean, and diverged to the west of the Kerguelen Plateau (∼40°E). One particle continued its backward journey following the ACC, eventually crossing it southward into the Antarctic region, during its second loop around the Southern Ocean. The second particle was entrained into, and looped around, the Brazil-Malvinas Confluence, before joining the Brazil Current and leaving the model domain toward subtropical latitudes. The two particles exhibited contrasting histories in terms of their ventilation. For the southern particle, 20 years elapsed from its release in the SAMW formation region to the last time it was observed in the surface mixed layer (which represents the time of the earliest upwelling of deep waters into the mixed layer in a forward sense). Of these 20 years, the particle spent 8 years in the mixed layer, experiencing extensive contact with the overlying atmosphere. In contrast, the northern particle followed mostly a subsurface pathway during its 16 years backward transit between the SAMW formation region and the subtropical gyre. This particle outcropped in the mixed layer only locally in the Pacific SAMW formation region, within one year of release.

The contribution of the subtropical and Antarctic water sources to the different SAMW pools is investigated in Fig. 3, which shows the proportion of particles in each frontal zone as a function of backward (negative) time since release, for the four SAMW formation regions. At time zero, particles were released mostly within the sub-Antarctic Zone, although a significant fraction ($\gtrsim$50%) of the Indian Ocean particles were released within the Subtropical Zone (Fig. 3), since the SAMW formation region there extends northward across the Subtropical Front delineated following the definition of Orsi et al. (1995) (Fig. 1). Within the first two years since release, the fraction of particles located north of the Subtropical Zone reached ∼70% in the central and east Indian regions (Fig. 3a,b), and a growing number of particles left the model domain across the northern boundary defined at 30°S. More than half of the subtropical particles left the model domain within 5 years, with almost all particles leaving within 15 years.

Concurrently, a smaller group of particles progressively crossed the ACC fronts southward, with most of the crossings taking place in the first 10-15 years. At 25 years since release, the distribution of particles in the frontal zones stabilised, with 70% of the particles having exited the model domain into the subtropics, and 25% of the particles located south of the sub-Antarctic Front. The proportion of particles in different frontal regions after 25 years was similar between the two Indian Ocean regions (Fig. 3a,b). Thus, the majority of the SAMWs formed in the Indian Ocean are supplied from the subtropics.

In the Pacific SAMW formation regions, all particles were located within the sub-Antarctic Zone at release, and 50% of the particles were found to the south of the sub-Antarctic Front after 25 years of tracking. A significant fraction of this 50% was located in the Antarctic Zone, south of the ACC's southern boundary. Finally, ∼30% of particles were found at subtropical latitudes after 25 years of backward tracking (Fig. 3c,d)

To gain further insight into the origin of subtropical waters entering the Southern Ocean, we classified the particles as a function of their location within the continental boundary regions depicted by polygons in Fig. 1. Different SAMW formation areas were connected with different boundary regions on different time scales (Fig. 4). About half

of the particles contributing to SAMW formation in the central Indian Ocean entered (in a forward sense) the model domain in the Agulhas Current (Fig. 4a). The transit time between the Agulhas Current region and the Indian SAMW formation region was short, less than 2 years, for most of these particles. Fewer particles (∼10%) linked the central Indian SAMW formation area with the South Atlantic western boundary region (the Brazil Current), on longer time scales of 3-7 years. The most important source of east Indian SAMW was the East Australian Current, with smaller contributions from the Agulhas Current, the Brazil Current, and the Leeuwin Current along West Australia (Fig. 4b). The relatively small fraction of subtropical waters feeding the Pacific SAMWs entered the model domain mainly via the Agulhas and Brazil currents, with similar contributions of 10-15% and transit times of 5-10 years (Fig. 4c,d). There was a smaller contribution from the East Australian Current (Fig. 4c,d). Some of the particles reaching the central Pacific SAMWs interacted with the boundary currents flowing along the eastern coast of New Zealand, but did not use that route to travel from the subtropics (Fig. 4c).

In subsequent descriptions, we classify the particles into two main pathways, the northern and southern pathways, for particles whose positions at the end of the backward simulation were located to the north or south of the sub-Antarctic Front, respectively.

3.2 Degree of exposure of SAMW sources to the surface mixed layer

The importance of surface fluxes for transforming source waters into SAMWs is controlled to a large extent by the time spent by these waters in the mixed layer, in direct contact with the atmosphere. The degree of mixed layer exposure (i.e., ventilation) along the different pathways and across SAMW formation regions is illustrated in Figs. 5 and 6. These figures show the distributions of locations at which particles were found within the mixed layer, and of locations at which particles were last observed within the mixed layer in the backward simulation (which represents the time of earliest upwelling into the mixed layer in a forward sense), respectively. These figures, and Table 1, also display the mean transit times in the model domain and mean total time of exposure to the mixed layer (Fig 5), as well as the mean time between SAMW formation and earliest upwelling into the mixed layer (Fig 6).

Particles following the northern subtropical pathway have relatively short transits within the model domain of 6.8 and 8.6 years for the central and east Indian SAMWs, respectively, but longer at 16.1 and 16.6 years for the central and east Pacific SAMWs (Fig. 5a-d, Table 1). For the northern particles, the earliest upwelling to the mixed layer occurred either within the western boundary current regions, or within (or immediately upstream of) their respective SAMW formation areas (Fig. 6a-d). The mean times from earliest upwelling to SAMW formation were 4.7-6.2 years and 10.1-9.5 years, in the Indian and Pacific regions, respectively (Table 1). Northern waters spent on average 1.2-1.7 years in the mixed layer, representing 17% and 10% of their transit time in the Indian and Pacific Oceans, respectively (Table 1). Consistent with the locations of earliest upwelling, exposure to the mixed layer was mostly local or closely upstream of the respective SAMW formation areas. This coincidence was particularly obvious for the east Pacific SAMWs (Fig. 5d).

In contrast, the southern sources of SAMWs remained within the model domain for the entire duration (25 years) of the back-tracking experiment (Fig. 5e-h, Table 1). Typically, the particles first upwelled into the mixed layer 15 years prior to release (in a forward sense), and the upwelling locations were concentrated along the ACC's southern flank (Fig. 6e-h). The distribution of earliest upwelling locations was zonally asymmetric, with most particles upwelling around regions of topographic steering of the ACC: the Southwest Indian Ridge (∼0-50°E), the Kerguelen Plateau (∼70–100°E), the Macquarie Ridge (∼150–180°E), and to a lesser degree the Pacific–Antarctic Ridge (∼180–

200°E). In contrast, upwelling was minimal in the Pacific Ocean, east of 200°E. These results are in line with previous model investigations of Southern Ocean upwelling (Viglione & Thompson, 2016; Tamsitt et al., 2017; Drake et al., 2018; Brady et al., 2021; Yung et al., 2022; Youngs & Flierl, 2023).

The particles of Southern origin experienced a more extensive exposure to the mixed layer along their pathways compared to northern-sourced particles (Fig. 5e-h). The southern sources of Indian and Pacific SAMWs spent on average 6.2 years and 5.0 years within the mixed layer, respectively, representing 25% and 20% of their transit times (Table 1).

3.3 Water mass transformations: property changes and drivers

We now investigate the thermohaline transformations that occur along the particle pathways, leading to the formation of the different varieties of SAMW from their respective sources, and assess the contributions of surface fluxes and subsurface ocean mixing to these transformations.

On average, particles at their release location (i.e. at the time that they become SAMW) were warmer and lighter than their southern sources, and cooler and denser than their northern sources (Fig. 7a,i). Changes in salinity were more complex, with Indian SAMWs being fresher than their northern sources, but saltier than their southern sources, whilst Pacific SAMWs were fresher than both of their sources (Fig. 7e). Overall, Pacific SAMWs were cooler, fresher and denser than their Indian counterparts, consistent with observations (McCartney, 1977; Herraiz-Borreguero & Rintoul, 2011; Bushinsky & Cerovečki, 2023). Southern sources for all SAMW formation regions exhibited a comparably small property variability, both within and across regions, with values of $\Theta \sim 1.6$°C and $S_A \sim 34.6$ g kg^{-1}, consistent with those of CDW. This result confirms that CDW is the primary southern source for all SAMW varieties. In contrast, northern sources displayed more ample variability, both within and across regions, being on average warmer, saltier and lighter in the Indian Ocean, compared to the Pacific Ocean (Fig. 7a,e,i).

The cooling experienced by northern-sourced particles amounted to -(3.5-3.6)°C and -(5.2-5.7)°C, in the Indian and Pacific oceans, respectively (Fig. 7b). This cooling was driven by a combination of surface fluxes and mixing. Surface cooling was more intense in the Indian Ocean (-2.3°C) than in the Pacific Ocean (-1.4°C) (Fig. 7b), but mixing more intense in the Pacific (-4°C) than in the Indian Ocean (-1.3°C). In contrast, northern precursors of SAMW were freshened (by -0.2 g kg^{-1} and -0.7 g kg^{-1} in the Indian and Pacific oceans, respectively) exclusively by mixing, only weakly opposed by surface freshwater fluxes in the Indian Ocean (Fig. 7f). Heat fluxes were the main drivers of densification along the northern pathway, by +(0.6-0.7) kg m^{-3} and +(0.3-0.4) kg m^{-3} in the Indian and Pacific oceans, respectively (Fig. 7j). Densification via cooling was due mainly by surface fluxes and, to a lesser extent, mixing, which was most substantial in the Pacific.

SAMW precursors in the southern pathway were warmed by +(8.4-9.3)°C and +(3.5-4.3)°C in the Indian and Pacific oceans, respectively. Such warming resulted from both surface heat fluxes and mixing, with the latter being generally dominant (Fig. 7c). Surface fluxes and mixing had strongly opposing effects on salinity for this route (Fig. 7g). Surface freshwater fluxes drove a rather uniform freshening by -1 g kg^{-1} across SAMW formation regions, which was opposed by a mixing-driven salinification of +(1.4-1.5) g kg^{-1} and +(0.6-0.7) g kg^{-1}, in the Indian and Pacific oceans, respectively. The net result was a salinification by +0.4 g kg^{-1} along the southern pathways supplying Indian SAMWs, and a freshening by -(0.2-0.3) g kg^{-1} for Pacific SAMWs. Surface fluxes of heat and freshwater lightened southern source waters, but salinity mixing moderated the density changes, which amounted to -0.8 kg m^{-3} and -0.6 kg m^{-3} in the Indian and Pacific oceans, respectively (Fig. 7k).

Considering the two groups of source water masses together gives insights into the nature of the different SAMW flavours, in terms of their role in climate as net sources of heat and freshwater to the atmosphere. Indian SAMWs are cooler than the average of their northern and southern sources by -(0.5-0.8)°C, and this cooling is driven mainly by surface heat fluxes, which cool source waters by -(0.7-0.9)°C, opposed by a smaller mixing-driven warming of +(0.1-0.2)°C (Fig. 7d). Pacific SAMWs are also cooler than the average of both sources by -(0.6-1.1)°C, but the cooling is primarily driven by mixing at -(0.8-0.9)°C, with little net loss or gain from the atmosphere. All SAMWs are also made fresher than the mean of the two sources by surface freshwater fluxes, but to a much larger extent in the Pacific, at -(0.5-0.6) g kg^{-1}, than in the Indian Ocean, at -0.1 g kg^{-1} (Fig. 7h).

In summary, the formation of Indian SAMWs – operating mainly along the subtropical pathway – results in an overall release of heat to the atmosphere and a relatively small net uptake of freshwater, whilst the formation of Pacific SAMWs – operating mainly along the Antarctic pathway – involves only small net heat exchange with the atmosphere, but a strong net freshwater uptake. Therefore, the relative importance of the northern and southern sources confers the different SAMWs pools with a distinct climatic role.

3.4 Water mass transformations: sequence of transformation processes along pathways

The water mass transformations documented above did not take place uniformly along particle trajectories. Rather, changes in Θ, S and σ_Θ (Fig. 8) by surface fluxes and mixing were localised in geographical (Fig. 9) and property spaces (Fig. 10). Here, we exploit this separation to disentangle the sequence of transformations leading to SAMW formation along the different pathways and for the different formation regions.

Maps and temperature-salinity diagrams in Figs. 9-10 are used to illustrate the sequence of transformations for northern and southern precursors of SAMW formation. In the manuscript, we focus on the easternmost SAMW pool in the Pacific to illustrate those transformations. Equivalent figures for the westernmost pool of the central Indian Ocean are presented as supplementary information (Supp. Figs. S1-S2). In these figures, changes in σ_Θ are represented by red-blue colours, and Θ and S_A changes are indicated by vectors in the y and x directions, respectively. In the geographical maps (Fig.9), the Θ and S_A changes have been scaled by the thermal expansion (α) and haline contraction (β) coefficients (Fig. 8), a representation that serves to highlight locations of diapycnal versus isopycnal transformations. Isopycnal transformations are represented by arrows at angles of 45° and -135° to the horizontal. Arrows at 45° indicate a density-compensated warming and salinification, while arrows at -135° indicate a density-compensated cooling and freshening (Fig. 8).

3.4.1 Transformation in the subtropical pathway

In the northern pathway, subtropical thermocline waters first undergo atmospheric cooling within western boundary currents (Fig. 10b). This cooling is mostly apparent in the Brazil Current region in the case of east Pacific SAMW (Fig. 9c), and very prominent in the Agulhas Current and Retroflection regions in the case of central Indian SAMW (Supp. Figs. S1c, S2b). Atmospheric cooling continues intermittently as the particles occasionally emerge into the mixed layer along their transit in the ACC, resulting also in densification (Figs. 9c, 10b).

Subsurface mixing all along the ACC contributes substantially to making subtropical source waters cooler and fresher (Figs. 9d, 10c). Such mixing operates mostly along isopycnal surfaces, which is consistent with the identification of the ACC as a hotspot for eddy stirring and isopycnal mixing (Naveira Garabato et al., 2016), and with the role

of cross-frontal exchange in the progressive cooling and freshening of SAMWs, and their precursors, along the path of the ACC, as described in previous studies (Sloyan & Rintoul, 2001; Holte et al., 2013). Along with isopycnal transformations, there is also substantial residual densification (Fig. 9d), which could be induced by a combination of cabbeling due to isopycnal stirring and direct diapycnal mixing (Groeskamp, Abernathey, & Klocker, 2016). In general, mixing-driven transformations are more important relative to surface fluxes for Pacific SAMWs, compared to Indian SAMWs (Fig. 7, Supp. Fig. S1c,d). We attribute this to the longer transit of Pacific SAMWs' northern sources within the ACC, which allows for more extensive mixing, and the relatively warm temperatures of the Agulhas Current waters that feed Indian SAMWs formation, which result in stronger surface cooling (Supp. Figs. S1c, S2b).

The final step of the transformation of subtropical source waters into SAMWs involves atmospheric cooling and densification close to and within the formation region (Figs. 9c, 10b). Local surface-driven densification entails convective vertical mixing between saltier subsurface waters of subtropical origin and fresher surface Antarctic waters, which are advected cross into the Sub-Antarctic Zone through Ekman transport (Rintoul & England, 2002) (see also Fernández Castro et al. (2022)). Such vertical mixing contributes to further freshening of the subtropical sources (Fig. 10c), which is more clearly visible for the central Indian Ocean (left-pointing arrows in Supp. Fig. S2c).

3.4.2 Transformation in the Antarctic pathway

Source waters in the southern pathway originate at $\Theta \approx 1.6$°C and $S_A \approx 34.6$ g kg^{-1}, consistent with CDW properties (Fig. 10d, Supp. Fig. S2d). The first step of the transformation is a drastic salinity reduction to <34.0 g kg^{-1} at near-constant temperature as the southern waters become lighter, moving toward the density classes of Antarctic surface waters (Fig. 10d). The strong initial salinity decrease is driven by mixing, rather than surface fluxes (Fig. 10e,f). We attribute this transformation to diapycnal mixing of subsurface CDW with the relatively fresh surface layers of the Southern Ocean, and eventual entrainment of CDW into the surface mixed layer, in line with previous modelling studies of the Southern Ocean overturning (Iudicone, Madec, et al., 2008; Iudicone, Speich, et al., 2008).

Once in the mixed layer, southern waters experience net surface warming, freshening and lightening (Figs. 9f,g, 10d,e). This transformation follows two distinct branches: a warming branch, and a first-cooling-then-warming branch. Waters in the warming branch upwell around and within the ACC (not shown), and directly experience net surface warming and freshening. Waters in the latter branch upwell mostly to the south of the ACC, in the Antarctic region. They first experience widespread atmospheric cooling and freshening (Fig. 9g), reducing Θ to negative values (Fig. 10e). As these waters move northward in the Ekman layer, they eventually reach net-warming latitudes around the ACC (Fig. 9g), and rejoin waters from the warming branch (Fig.10d,e).

Surface fluxes therefore cause waters in the southern pathway to reach similar temperatures to the corresponding SAMW variety, but much lower salinities, below 34 g kg^{-1} (Fig. 10e). Two processes contribute to the required salinification to transform them into SAMWs: subsurface isopycnal mixing within the ACC –again signaling the importance of cross-frontal exchange (Holte et al., 2013)–, and entrainment of saltier subsurface waters when particles are in the mixed layer (Figs. 9h, 10f). The entrainment of saltier subsurface waters is more intense at, and immediately upstream of, the SAMW formation regions (right-pointing arrows in Fig. 9h), and occurs concomitantly with strong surface cooling (Fig. 9g). Cooling at the SAMW formation regions is the final step of the transformation, which makes the surface waters dense enough to become SAMWs (Figs. 9g, 10e).

4 Summary and discussion

In this work, we used a virtual particle-tracking experiment in B-SOSE to investigate the sources of SAMWs, and the pathways and processes leading to SAMW formation in deep mixed layers of the Indian and Pacific oceans. Our analysis confirmed the occurrence of two contrasting sources of SAMWs (Fig. 11, and see also Fig. 2): an Antarctic source linked to the upwelling of colder and denser CDW, and a subtropical source comprising warmer, saltier and lighter thermocline waters. Our results shed light on the long-outstanding dichotomy regarding the origin of SAMWs and their role in the Southern Ocean overturning circulation, in which SAMW is regarded as either part of the global overturning's upper cell (Speer et al., 2000; Marshall & Speer, 2012; Abernathey et al., 2016), as the lower limb of a shallower subtropical overturning cell (McCartney, 1977), or as taking part in both deep and shallow overturning cells (Sloyan & Rintoul, 2001; Talley, 2003; Iudicone, Speich, et al., 2008; Iudicone et al., 2011). In the first interpretation, SAMWs originate from lightening of upwelled CDW, whereas in the second view, SAMWs result from cooling of subtropical waters flowing along the ACC (McCartney, 1977; Iudicone et al., 2011; Holte et al., 2012; Fernández Castro et al., 2022). We show that both sources contribute to SAMW formation, suggesting an intimate link of SAMWs with both the global (Döös et al., 2012; Iudicone, Speich, et al., 2008) and Southern Hemisphere's subtropical (Sloyan & Rintoul, 2001; Talley, 2003) overturning cells.

One of our main results is the contrast in the relative contributions of subtropical and Antarctic waters to the formation of different SAMW pools in the Indian and Pacific oceans and, therefore, their role in the overturning cells. Subtropical precursors are dominant for the Indian Ocean SAMWs (70-75% of the virtual particles), and less important (<40%) for Pacific SAMWs. This contrast explains, together with some differences in surface fluxes and interior mixing, why Indian SAMW varieties are warmer and saltier than their Pacific counterparts, as long noted in observations (McCartney, 1977; Sallée et al., 2010; Herraiz-Borreguero & Rintoul, 2011; Bushinsky & Cerovečki, 2023). Therefore, the eastward decrease in temperature and salinity across SAMWs pools should not be regarded exclusively as the result of a continuous transformation by surface fluxes as these waters flow eastward along the northern flank of the ACC, as sometimes implied (McCartney, 1977). In fact, our results suggest a rather moderate degree of surface ventilation of East Pacific SAMW's northern sources as they flow along the ACC (Figs. 5d, 9c). Although the SAMW varieties in the Indian and Pacific oceans are partly connected via ACC transport and transformations occurring there (mainly through interior mixing); they are also distinct water masses in terms of their primary sources, and play different roles in the global and subtropical circulation cells. Indian SAMWs are more closely related to the subtropical cell, while Pacific SAMWs are more closely related to CDW upwelling and the global overturning cell.

The subtropical and Antarctic sources of SAMWs follow contrasting pathways, with differing travel time scales and degrees of ventilation (i.e. exposure to the surface mixed layer) (Fig. 11). Subtropical waters enter the ACC in the western boundary regions of the Brazil, Agulhas and East Australian currents. These waters experience relatively short transits within the Southern Ocean (particularly for the Indian SAMWs, $\lesssim 5$ years) and only a brief exposure to the mixed layer ($\sim$1.5 years, mostly local to the SAMW formation regions). In contrast, Antarctic source waters experience longer transits in the upper Southern Ocean (~ 15 years), during which they interact extensively with the atmosphere, spending over 5 years in the mixed layer.

Due to the different trajectories, degrees of ventilation and properties at source, the two pathways of SAMW formation are characterised by contrasting water mass transformations driven, to different degrees, by surface heat and freshwater fluxes and interior mixing. Subtropical surface and thermocline waters joining the ACC from western boundary currents are transformed into cooler, fresher and denser SAMWs by surface heat fluxes (cooling, densification) and interior mixing (cooling and freshening) (Figs. 11,

7). Whilst surface fluxes account for cooling and densification, as previously described (McCartney, 1977; Iudicone, Speich, et al., 2008; Tamsitt et al., 2020), our analysis shows that interior mixing drives the observed net freshening.

Antarctic source waters, originating in CDW upwelling, are made warmer and lighter by surface heat and freshwater fluxes to form SAMWs (Figs. 11, 7). This is consistent with the conventional view of the Southern Ocean overturning circulation, whereby a fraction of the upwelled CDW volume experiences atmospheric and sea ice-induced lightening to join the northward-flowing shallow branch of the global overturning as Antarctic Intermediate Water and SAMWs (Abernathey et al., 2016; Evans et al., 2018; Pellichero et al., 2018). Our analysis also highlights the role of interior mixing, which reinforces surface warming but opposes surface freshening, resulting in a net mixing-driven densification, consistent with previous modelling studies (Iudicone, Madec, et al., 2008; Cerovečki et al., 2013; Abernathey et al., 2016).

Using Lagrangian trajectories, we mapped surface and interior fluxes onto geographical and property spaces, revealing the sequence of processes driving the formation of the different SAMW varieties from their subtropical and Antarctic precursors. Due to the limited exposure of subtropical source waters to the mixed layer, surface-driven cooling occurs only in two localised regions: within the southward-flowing western boundary currents, and within or immediately upstream of the SAMW formation regions (Fig. 11). Elsewhere, subtropical-sourced waters transit toward SAMW formation regions mostly in subsurface layers of the ACC, where they mix with cooler and fresher waters along isopycnals (Sloyan & Rintoul, 2001; Holte et al., 2013). Mixing-driven freshening and cooling is more important for Pacific SAMWs than for their Indian counterparts, due to the longer transit times of these waters within the ACC (Figs. 9b, S1b).

In the southern pathway, CDW-sourced waters are initially freshened through mixing with surface waters upon entrainment into the mixed layer (Fig. 11), as noted by Iudicone, Speich, et al. (2008). During their transit in the surface Southern Ocean, upwelled waters experience net warming (after some initial cooling) and freshening via surface fluxes, as they are advected northward towards and within the ACC, consistent with Abernathey et al. (2016); Evans et al. (2018). These fluxes drive a transformation that would eventually create waters that are lighter and fresher than the corresponding SAMWs. Whilst subsequent densification occurs mainly via surface heat loss close to the formation region, the required salinification is achieved through mixing via two distinct processes: isopycnal mixing with northern waters within the ACC, and vertical mixing with saltier subsurface waters (CDW in the Antarctic region, and subtropical waters within and north of the ACC) (Fernández Castro et al., 2022)). Importantly, the magnitude of mixing-driven salinification imprints into the different character of Indian and Pacific SAMWs, which are saltier and fresher than CDW, respectively.

4.1 Limitations

It must be noted that our findings are subject to uncertainties and limitations inherent to modelling studies. Our chosen model, B-SOSE, assimilates a broad range of ocean observations and has been extensively validated (Mazloff et al., 2010; Cerovečki et al., 2013; Verdy & Mazloff, 2017; Bushinsky & Cerovečki, 2023), which minimises but does not eliminate biases. For example, our B-SOSE iteration shows a region of deep mixed layers immediately south of Tasmania, which is not prominent in Argo climatologies (Li et al., 2021) or earlier SOSE iterations (Cerovečki & Mazloff, 2016). If this feature indicates a model bias, it could also imply biases in the proportion of source waters for the East Indian SAMW.

A key source of uncertainty is the representation of sub-grid mixing processes, both in the original B-SOSE simulation –which is known to affect tracer distributions and fluxes (Ellison et al., 2023), potentially impacting our water mass transformation estimates–

, as well as in the representation of surface-enhanced mixing in the Lagrangian simulation, where periodic reshuffling is introduced. Notably, our results proved to be highly robust to this approach (see Methods).

Despite these limitations, our findings generally align with previous modelling and observational studies of Southern Ocean circulation and water mass transformations, which indicate the co-existence of southern and northern sources for SAMWs (e.g., Sloyan et al. (2010); Iudicone, Speich, et al. (2008)). We complement those studies by quantifying the relative contributions of source waters to different SAMW pools and their role in the exchange of heat and freshwater with the atmosphere. Our key result –concerning the general dominance of subtropical and Circumpolar Deep Water sources in the Indian and Pacific oceans, respectively– appears robust and highly plausible in light of the observed property contrasts between SAMW pools (Sallée et al., 2010; Herraiz-Borreguero & Rintoul, 2011; Bushinsky & Cerovečki, 2023). Similar experiments with different models in future work would help to further gauge the robustness of our results.

5 Wider Implications

In this work we performed a Lagrangian tracking experiment to investigate the sources, pathways and drivers of sub-Antarctic Mode Waters (SAMWs) formation. We show that SAMWs form due to the combination of warming, freshening and lightening of dense Circumpolar Deep Waters by air-sea and ice-sea fluxes (Speer et al., 2000; Marshall & Speer, 2012; Abernathey et al., 2016), and atmospheric cooling and densification of southward-flowing subtropical waters (McCartney, 1977; Sloyan et al., 2010; Iudicone et al., 2011; Talley, 2013). The relative contribution of the subtropical sources is different in different SAMW pools, being dominant in Indian Ocean SAMWs and secondary in Pacific Ocean SAMWs.

The subtropical and Antarctic pathways for SAMWs are characterised by opposing surface heat fluxes taking place in geographically distant locations: subtropical waters lose heat to the atmosphere in western boundary currents and SAMW formation regions, whereas Antarctic waters experience warming at the core and southern edge of the Antarctic Circumpolar Current. This result points to a different role of the two main SAMW formation pathways in atmosphere-ocean heat exchange. It is also consistent with results from adjoint modelling experiments showing complex sensitivities of SAMW formation rates and properties to perturbations in external forcing both to the north and south of the ACC (Boland et al., 2021). Further, the prevalence of northern and southern sources for Indian and Pacific SAMW varieties, respectively, has consequences for their overall role as net sources or sinks of atmospheric heat and freshwater. Indian SAMW formation results in a net release of heat to the atmosphere, while Pacific SAMW formation entails a strong ocean uptake of freshwater associated with comparably small net heat fluxes. Therefore, the different SAMW pools may play a distinct role in the climate system.

Our findings may also have important implications for our understanding of the role of SAMWs as sinks of anthropogenic heat and carbon dioxide, and as conveyors of nutrients to northern latitudes. The prevalence of subtropical sources implies that Indian SAMWs likely behave as net atmospheric carbon sinks, since the uptake of carbon dioxide in the Southern Ocean occurs primarily north of the ACC and in the western boundaries (Iudicone et al., 2011; Gruber et al., 2019; Prend et al., 2022; Gray, 2024). Southern-sourced Pacific SAMWs are instead likely carbon sources to the atmosphere, since the upwelling of CDW involves a strong out-gassing within and south of the Antarctic Circumpolar Current (Gray et al., 2018; Prend et al., 2022). The different SAMW pools are characterised by eastward-increasing nutrient concentrations between the Indian and Pacific Oceans (Fernández Castro et al., 2022; Bushinsky & Cerovečki, 2023). This increase is consistent with lower temperature and salinity values, and the larger con-

tribution of nutrient-poor subtropical waters in the Indian Ocean. Therefore, strong interannual-to-interdecadal changes in the volume production of different SAMW varieties, as identified in observations (Gao et al., 2018; Meijers et al., 2019; Xu et al., 2021; Cerovečki & Haumann, 2023), could be associated with significant variability in the Southern Ocean carbon sink and in the degree of fertilisation of the northern ocean basins (Sarmiento et al., 2004; Hauck et al., 2018). Further, temporal changes in the relative contributions of subtropical and Antarctic sources within each pool, which are largely unknown, could also impact the exchange of heat and carbon with the atmosphere, as well as nutrient supply to lower latitudes. A detailed quantification of the biogeochemical transformations along SAMW pathways, and their interannual and decadal variability, would be required to define the sensitivity of nutrient redistribution and carbon sequestration by SAMW to climatic forcing perturbations.

Open Research Section

Original data from the iteration 139 of B-SOSE can downloaded from `http://sose.ucsd.edu/SO6/ITER139/`. The particle tracking software, OceanParcels, is available at `https://oceanparcels.org/`. The particle trajectories used in this study alongside Python code and notebooks used for data analysis are available at Fernández Castro et al. (2025). We are grateful to Claudia Ofelio for her artwork on Figure 11).

Conflict of Interest Statement

The authors declare that they have no conflicts of interest.

Acknowledgments

This research was funded by European Union's Horizon 2020 research and innovation program under the Marie Skłodowska-Curie grant agreement No. 834330 (SO-CUP) to BFC. BFC is also supported by NERC grants NE/W009528/1 and NE/Y002709/1. ACNG acknowledges U.K. Research and Innovation guarantee funding for a European Research Council Advanced Grant (EP/X025136/1).

References

Abernathey, R. P., Cerovecki, I., Holland, P. R., Newsom, E., Mazloff, M., & Talley, L. D. (2016). Water-mass transformation by sea ice in the upper branch of the Southern Ocean overturning. *Nature Geoscience*, *9*(8), 596–601. doi: 10.1038/ngeo2749

Boland, E. J. D., Jones, D. C., Meijers, A. J. S., Forget, G., & Josey, S. A. (2021). Local and Remote Influences on the Heat Content of Southern Ocean Mode Water Formation Regions. *Journal of Geophysical Research: Oceans*, *126*(4). doi: 10.1029/2020JC016585

Brady, R. X., Maltrud, M. E., Wolfram, P. J., Drake, H. F., & Lovenduski, N. S. (2021). The Influence of Ocean Topography on the Upwelling of Carbon in the Southern Ocean. *Geophysical Research Letters*, *48*(19). doi: 10.1029/2021GL095088

Bushinsky, S. M., & Cerovečki, I. (2023). Subantarctic Mode Water Biogeochemical Formation Properties and Interannual Variability. *AGU Advances*, *4*(2). doi: 10.1029/2022AV000722

Cerovečki, I., & Haumann, F. A. (2023). Decadal Reorganization of Subantarctic Mode Water. *Geophysical Research Letters*, *50*(14), e2022GL102148. doi: 10.1029/2022GL102148

Cerovečki, I., & Mazloff, M. R. (2016). The Spatiotemporal Structure of Diabatic Processes Governing the Evolution of Subantarctic Mode Water in the

Southern Ocean. *Journal of Physical Oceanography*, *46*(2), 683–710. doi: 10.1175/JPO-D-14-0243.1

Cerovečki, I., Meijers, A. J. S., Mazloff, M. R., Gille, S. T., Tamsitt, V. M., & Holland, P. R. (2019). The Effects of Enhanced Sea Ice Export from the Ross Sea on Recent Cooling and Freshening of the Southeast Pacific. *Journal of Climate*, *32*(7), 2013–2035. doi: 10.1175/JCLI-D-18-0205.1

Cerovečki, I., Talley, L. D., Mazloff, M. R., & Maze, G. (2013). Subantarctic Mode Water Formation, Destruction, and Export in the Eddy-Permitting Southern Ocean State Estimate. *Journal of Physical Oceanography*, *43*(7), 1485–1511. doi: 10.1175/JPO-D-12-0121.1

Chen, H., Haumann, F. A., Talley, L. D., Johnson, K. S., & Sarmiento, J. L. (2022). The Deep Ocean's Carbon Exhaust. *Global Biogeochemical Cycles*, *36*(7). doi: 10.1029/2021GB007156

Dee, D. P., Uppala, S. M., Simmons, A. J., Berrisford, P., Poli, P., Kobayashi, S., ... Vitart, F. (2011). The ERA-Interim reanalysis: configuration and performance of the data assimilation system. *Quarterly Journal of the Royal Meteorological Society*, *137*(656), 553–597. doi: 10.1002/qj.828

Delandmeter, P., & van Sebille, E. (2019). The Parcels v2.0 Lagrangian framework: new field interpolation schemes. *Geoscientific Model Development*, *12*(8), 3571–3584. doi: 10.5194/gmd-12-3571-2019

Drake, H. F., Morrison, A. K., Griffies, S. M., Sarmiento, J. L., Weijer, W., & Gray, A. R. (2018). Lagrangian Timescales of Southern Ocean Upwelling in a Hierarchy of Model Resolutions. *Geophysical Research Letters*, *45*(2), 891–898. doi: 10.1002/2017GL076045

Döös, K., Nilsson, J., Nycander, J., Brodeau, L., & Ballarotta, M. (2012). The World Ocean Thermohaline Circulation*. *Journal of Physical Oceanography*, *42*(9), 1445–1460. doi: 10.1175/JPO-D-11-0163.1

Ellison, E., Mashayek, A., & Mazloff, M. (2023). The Sensitivity of Southern Ocean Air-Sea Carbon Fluxes to Background Turbulent Diapycnal Mixing Variability. *Journal of Geophysical Research: Oceans*, e2023JC019756. doi: 10.1029/2023JC019756

Evans, D. G., Zika, J. D., Naveira Garabato, A. C., & Nurser, A. J. G. (2018). The Cold Transit of Southern Ocean Upwelling. *Geophysical Research Letters*, *45*(24). doi: 10.1029/2018GL079986

Fernández Castro, B., Mazloff, M., Williams, R. G., & Naveira Garabato, A. C. (2022). Subtropical Contribution to Sub-Antarctic Mode Waters. *Geophysical Research Letters*, *49*(11). doi: 10.1029/2021GL097560

Fernández Castro, B., Naveira Garabato, A. C., Mazloff, M., & Williams, R. (2025). *Data for "Sources, pathways and drivers of Sub-Antarctic Mode Water formation"*. Zenodo. doi: 10.5281/zenodo.14998365

Gao, L., Rintoul, S. R., & Yu, W. (2018). Recent wind-driven change in Subantarctic Mode Water and its impact on ocean heat storage. *Nature Climate Change*, *8*(1), 58–63. doi: 10.1038/s41558-017-0022-8

Gray, A. R. (2024). The Four-Dimensional Carbon Cycle of the Southern Ocean. *Annual Review of Marine Science*, *16*(1), 163–190. doi: 10.1146/annurev-marine-041923-104057

Gray, A. R., Johnson, K. S., Bushinsky, S. M., Riser, S. C., Russell, J. L., Talley, L. D., ... Sarmiento, J. L. (2018). Autonomous Biogeochemical Floats Detect Significant Carbon Dioxide Outgassing in the High-Latitude Southern Ocean. *Geophysical Research Letters*, *45*(17), 9049–9057. doi: 10.1029/2018GL078013

Groeskamp, S., Abernathey, R. P., & Klocker, A. (2016). Water mass transformation by cabbeling and thermobaricity. *Geophysical Research Letters*, *43*(20). doi: 10.1002/2016GL070860

Groeskamp, S., & Iudicone, D. (2018). The Effect of Air-Sea Flux Products, Short-

wave Radiation Depth Penetration, and Albedo on the Upper Ocean Overturning Circulation. *Geophysical Research Letters*, *45*(17), 9087–9097. doi: 10.1029/2018GL078442

Groeskamp, S., Lenton, A., Matear, R., Sloyan, B. M., & Langlais, C. (2016). Anthropogenic carbon in the ocean—Surface to interior connections. *Global Biogeochemical Cycles*, *30*(11), 1682–1698. doi: 10.1002/2016GB005476

Gruber, N., Landschützer, P., & Lovenduski, N. S. (2019). The Variable Southern Ocean Carbon Sink. *Annual Review of Marine Science*, *11*(1), 159–186. doi: 10.1146/annurev-marine-121916-063407

Hanawa, K., & Talley, L. D. (2001). Chapter 5.4 Mode waters. *International Geophysics*, *77*(C), 373–386. (ISBN: 0126413517) doi: 10.1016/S0074-6142(01)80129-7

Hauck, J., Lenton, A., Langlais, C., & Matear, R. (2018). The Fate of Carbon and Nutrients Exported Out of the Southern Ocean. *Global Biogeochemical Cycles*, *32*(10), 1556–1573. doi: 10.1029/2018GB005977

Herraiz-Borreguero, L., & Rintoul, S. R. (2011). Subantarctic mode water: distribution and circulation. *Ocean Dynamics*, *61*(1), 103–126. doi: 10.1007/s10236-010-0352-9

Holte, J. W., Talley, L. D., Chereskin, T. K., & Sloyan, B. M. (2012). The role of air-sea fluxes in Subantarctic Mode Water formation. *Journal of Geophysical Research: Oceans*, *117*(C3), C03040. doi: 10.1029/2011JC007798

Holte, J. W., Talley, L. D., Chereskin, T. K., & Sloyan, B. M. (2013). Subantarctic mode water in the southeast Pacific: Effect of exchange across the Subantarctic Front. *Journal of Geophysical Research: Oceans*, *118*(4), 2052–2066. doi: 10.1002/jgrc.20144

Iudicone, D., Madec, G., Blanke, B., & Speich, S. (2008). The Role of Southern Ocean Surface Forcings and Mixing in the Global Conveyor. *Journal of Physical Oceanography*, *38*(7), 1377–1400. doi: 10.1175/2008JPO3519.1

Iudicone, D., Rodgers, K. B., Stendardo, I., Aumont, O., Madec, G., Bopp, L., ... Ribera d'Alcala', M. (2011). Water masses as a unifying framework for understanding the Southern Ocean Carbon Cycle. *Biogeosciences*, *8*(5), 1031–1052. doi: 10.5194/bg-8-1031-2011

Iudicone, D., Speich, S., Madec, G., & Blanke, B. (2008). The Global Conveyor Belt from a Southern Ocean Perspective. *Journal of Physical Oceanography*, *38*(7), 1401–1425. doi: 10.1175/2007JPO3525.1

Jones, D. C., Meijers, A. J. S., Shuckburgh, E., Sallée, J.-B., Haynes, P., McAufield, E. K., & Mazloff, M. R. (2016). How does Subantarctic Mode Water ventilate the Southern Hemisphere subtropics? *Journal of Geophysical Research: Oceans*, *121*(9), 6558–6582. doi: 10.1002/2016JC011680

Lange, M., & van Sebille, E. (2017). Parcels v0.9: prototyping a Lagrangian ocean analysis framework for the petascale age. *Geoscientific Model Development*, *10*(11), 4175–4186. doi: 10.5194/gmd-10-4175-2017

Li, Z., England, M. H., Groeskamp, S., Cerovečki, I., & Luo, Y. (2021). The Origin and Fate of Subantarctic Mode Water in the Southern Ocean. *Journal of Physical Oceanography*. doi: 10.1175/JPO-D-20-0174.1

Marshall, J., & Speer, K. (2012). Closure of the meridional overturning circulation through Southern Ocean upwelling. *Nature Geoscience*, *5*(3), 171–180. doi: 10.1038/ngeo1391

Mazloff, M. R., Heimbach, P., & Wunsch, C. (2010). An Eddy-Permitting Southern Ocean State Estimate. *Journal of Physical Oceanography*, *40*(5), 880–899. doi: 10.1175/2009JPO4236.1

McCartney, M. S. (1977). Subantarctic mode water. *Journal of Marine Research*, *76*(3-4).

Meijers, A. J. S., Cerovečki, I., King, B. A., & Tamsitt, V. (2019). A See-Saw in Pacific Subantarctic Mode Water Formation Driven by Atmospheric Modes. *Geo-*

physical Research Letters, *46*(22), 13152–13160. doi: 10.1029/2019GL085280

Morrison, A. K., Waugh, D. W., Hogg, A. M., Jones, D. C., & Abernathey, R. P. (2022). Ventilation of the Southern Ocean Pycnocline. *Annual Review of Marine Science*, *14*(1), 405–430. doi: 10.1146/annurev-marine-010419-011012

Naveira Garabato, A. C., Polzin, K. L., Ferrari, R., Zika, J. D., & Forryan, A. (2016). A Microscale View of Mixing and Overturning across the Antarctic Circumpolar Current. *Journal of Physical Oceanography*, *46*(1), 233–254. doi: 10.1175/JPO-D-15-0025.1

Orsi, A. H., Whitworth, T., & Nowlin, W. D. (1995). On the meridional extent and fronts of the Antarctic Circumpolar Current. *Deep Sea Research Part I: Oceanographic Research Papers*, *42*(5), 641–673. doi: 10.1016/0967-0637(95)00021-W

Panassa, E., Santana-Casiano, J. M., González-Dávila, M., Hoppema, M., Van Heuven, S. M., Völker, C., ... Hauck, J. (2018). Variability of nutrients and carbon dioxide in the Antarctic Intermediate Water between 1990 and 2014. *Ocean Dynamics*, *68*(3), 295–308. doi: 10.1007/s10236-018-1131-2

Pellichero, V., Sallée, J.-B., Chapman, C. C., & Downes, S. M. (2018). The southern ocean meridional overturning in the sea-ice sector is driven by freshwater fluxes. *Nature Communications*, *9*(1), 1789. doi: 10.1038/s41467-018-04101-2

Prend, C. J., Gray, A. R., Talley, L. D., Gille, S. T., Haumann, F. A., Johnson, K. S., ... Sarmiento, J. L. (2022). Indo-Pacific Sector Dominates Southern Ocean Carbon Outgassing. *Global Biogeochemical Cycles*, *36*(7). doi: 10.1029/2021GB007226

Rintoul, S. R., & England, M. H. (2002). Ekman Transport Dominates Local Air–Sea Fluxes in Driving Variability of Subantarctic Mode Water. *Journal of Physical Oceanography*, *32*(5), 1308–1321. doi: 10.1175/1520-0485(2002)032⟨1308:ETDLAS⟩2.0.CO;2

Roemmich, D., Church, J., Gilson, J., Monselesan, D., Sutton, P., & Wijffels, S. (2015). Unabated planetary warming and its ocean structure since 2006. *Nature Climate Change*, *5*(3), 240–245. doi: 10.1038/nclimate2513

Sallée, J.-B., Speer, K., Rintoul, S., & Wijffels, S. (2010). Southern Ocean Thermocline Ventilation. *Journal of Physical Oceanography*, *40*(3), 509–529. doi: 10.1175/2009JPO4291.1

Sarmiento, J. L., Gruber, N., Brzezinski, M. A., & Dunne, J. P. (2004). High-latitude controls of thermocline nutrients and low latitude biological productivity. *Nature*, *427*(6969), 56–60. doi: 10.1038/nature02127

Sloyan, B. M., & Rintoul, S. R. (2001, April). Circulation, Renewal, and Modification of Antarctic Mode and Intermediate Water*. *Journal of Physical Oceanography*, *31*(4), 1005–1030. doi: 10.1175/1520-0485(2001)031⟨1005:CRAMOA⟩2.0.CO;2

Sloyan, B. M., Talley, L. D., Chereskin, T. K., Fine, R., & Holte, J. (2010). Antarctic Intermediate Water and Subantarctic Mode Water Formation in the Southeast Pacific: The Role of Turbulent Mixing. *Journal of Physical Oceanography*, *40*(7), 1558–1574. doi: 10.1175/2010JPO4114.1

Speer, K., Rintoul, S. R., & Sloyan, B. (2000). The Diabatic Deacon Cell*. *Journal of Physical Oceanography*, *30*(12), 3212–3222. doi: 10.1175/1520-0485(2000)030⟨3212:TDDC⟩2.0.CO;2

Talley, L. D. (2003). Shallow, Intermediate, and Deep Overturning Components of the Global Heat Budget. *Journal of Physical Oceanography*, *33*(3), 530–560. doi: 10.1175/1520-0485(2003)033⟨0530:SIADOC⟩2.0.CO;2

Talley, L. D. (2013). Closure of the Global Overturning Circulation Through the Indian, Pacific, and Southern Oceans: Schematics and Transports. *Oceanography*, *26*(1), 80–97. doi: 10.5670/oceanog.2013.07

Talley, L. D., Reid, J. L., & Robbins, P. E. (2003). Data-Based Meridional Overturning Streamfunctions for the Global Ocean. *Journal of Climate*, *16*(19),

3213–3226. doi: 10.1175/1520-0442(2003)016⟨3213:DMOSFT⟩2.0.CO;2

Tamsitt, V., Abernathey, R. P., Mazloff, M. R., Wang, J., & Talley, L. D. (2018). Transformation of Deep Water Masses Along Lagrangian Upwelling Pathways in the Southern Ocean. *Journal of Geophysical Research: Oceans*, *123*(3), 1994–2017. doi: 10.1002/2017JC013409

Tamsitt, V., Cerovečki, I., Josey, S. A., Gille, S. T., & Schulz, E. (2020). Mooring Observations of Air–Sea Heat Fluxes in Two Subantarctic Mode Water Formation Regions. *Journal of Climate*, *33*(7), 2757–2777. doi: 10.1175/JCLI-D-19-0653.1

Tamsitt, V., Drake, H. F., Morrison, A. K., Talley, L. D., Dufour, C. O., Gray, A. R., ... Weijer, W. (2017). Spiraling pathways of global deep waters to the surface of the Southern Ocean. *Nature Communications*, *8*(1), 172. doi: 10.1038/s41467-017-00197-0

Tamsitt, V., Talley, L. D., Mazloff, M. R., & Cerovečki, I. (2016). Zonal Variations in the Southern Ocean Heat Budget. *Journal of Climate*, *29*(18), 6563–6579. doi: 10.1175/JCLI-D-15-0630.1

Verdy, A., & Mazloff, M. R. (2017). A data assimilating model for estimating Southern Ocean biogeochemistry. *Journal of Geophysical Research: Oceans*, *122*(9), 6968–6988. doi: 10.1002/2016JC012650

Viglione, G. A., & Thompson, A. F. (2016). Lagrangian pathways of upwelling in the Southern Ocean. *Journal of Geophysical Research: Oceans*, *121*(8), 6295–6309. doi: 10.1002/2016JC011773

Wang, J., Mazloff, M. R., & Gille, S. T. (2014). Pathways of the Agulhas waters poleward of 29°S. *Journal of Geophysical Research: Oceans*, *119*(7), 4234–4250. doi: 10.1002/2014JC010049

Xu, L., Ding, Y., & Xie, S. (2021). Buoyancy and Wind Driven Changes in Subantarctic Mode Water During 2004–2019. *Geophysical Research Letters*, *48*(8). doi: 10.1029/2021GL092511

Youngs, M. K., & Flierl, G. R. (2023). Extending Residual-Mean Overturning Theory to the Topographically Localized Transport in the Southern Ocean. *Journal of Physical Oceanography*, *53*(8), 1901–1915. (Publisher: American Meteorological Society Section: Journal of Physical Oceanography) doi: 10.1175/JPO-D-22-0217.1

Yung, C. K., Morrison, A. K., & Hogg, A. M. (2022). Topographic Hotspots of Southern Ocean Eddy Upwelling. *Frontiers in Marine Science*, *9*, 855785. doi: 10.3389/fmars.2022.855785

Table 1. Mean time scales ± standard deviation of particle pathways leading to SAMW formation in the different regions. Time scales are calculated for the northern (N) and southern (S) pathways, with particles originating north and south of the sub-Antarctic Front, respectively.

Pathway	Region	Years in model domain	Years in mixed layer	Years since first upwelling
N	Central Indian	6.8±7.2	1.2±1.5	4.7±6.2
N	East Indian	8.7±7.8	1.5±1.6	6.2±6.9
N	Central Pacific	16.2±7.7	1.7±1.8	10.1±8.8
N	East Pacific	16.6±7.4	1.6±1.7	9.5±8.8
S	Central Indian	25.0±0.3	6.2±2.4	15.4±6.5
S	East Indian	25.0±0.4	6.2±2.4	16.0±6.3
S	Central Pacific	25.0±0.5	5.1±2.5	14.3±7.2
S	East Pacific	25.0±0.4	5.0±2.4	14.6±7.1

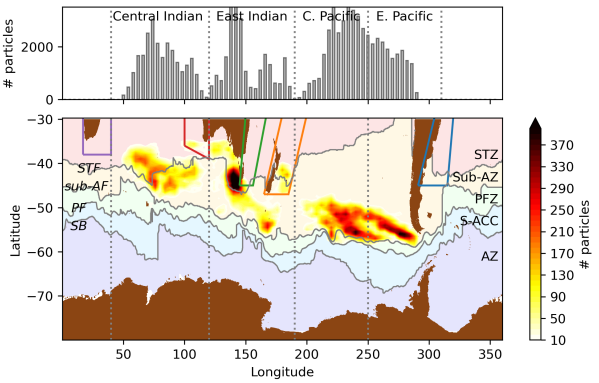

Figure 1. Distribution of the release locations for all particles in the Lagrangian simulation. The condition that mixed layer depth is greater than 300 m at the seeding location results in particle seeding exclusively within the SAMW formation regions during the winter season. Background colours represent the ACC fronts (left) frontal zones (right) delineated following the definition of Orsi et al. (1995). Boundary current regions are delimited by polygons: Agulhas Current (purple), South and West Australia (red), East Australian Current (green), New Zealand (orange), and Brazil Current (blue).

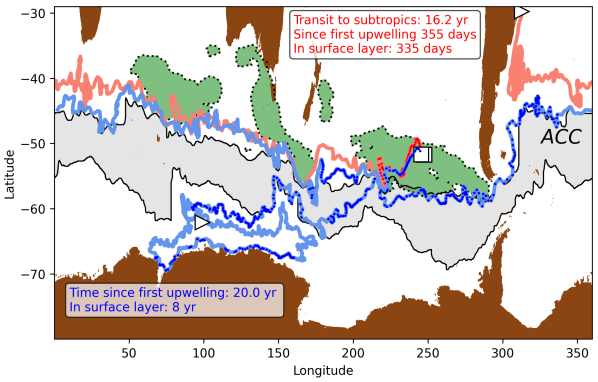

Figure 2. Examples of two backward trajectories for two particles released in neighbouring positions within the Pacific SAMW formation region. The contrasting northern (red) and southern (blue) pathways of water parcels contributing to the formation of SAMW are exemplified. The release positions are represented as squares and the positions at the end of the backward simulations are shown as right-facing triangles. Instances of particles being located within the surface mixed layer are highlighted with dark dots. Time before leaving the model domain towards the subtropics, time spent from first upwelling into the mixed layer and time spent within the mixed layer are reported for the two particles. The green shading delimit the location of particle releases within the SAMW formation regions, and the gray shading delimits the ACC meridional extent delimited by the Sub-Antarctic Front and the ACC's southern boundary.

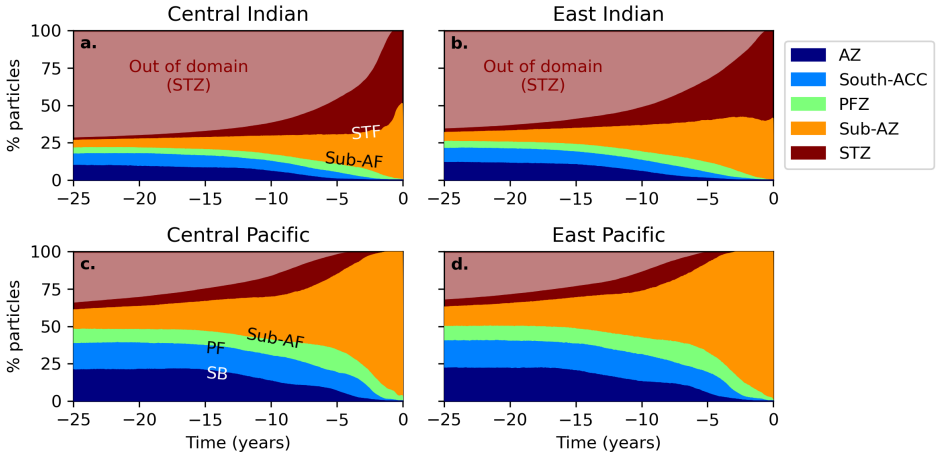

Figure 3. Distribution of particles across frontal zones as a function of backward time for particles originating in the different SAMW formation regions. Particles leaving the model domain (labeled out of domain) are accumulated such that the total number of particles is conserved. Out of domain particles should be considered as of subtropical origin, since they leave the model domain northward across 30°C within western boundary currents (WBC). A clear contrast between Indian and Pacific SAMWs is observed. Subtropical source waters are the primary component of Indian SAMWs (70-75%), and a secondary component of Pacific SAMWs (∼35%), which are largely sourced from particles originating south of the sub-Antarctic Front (50%).

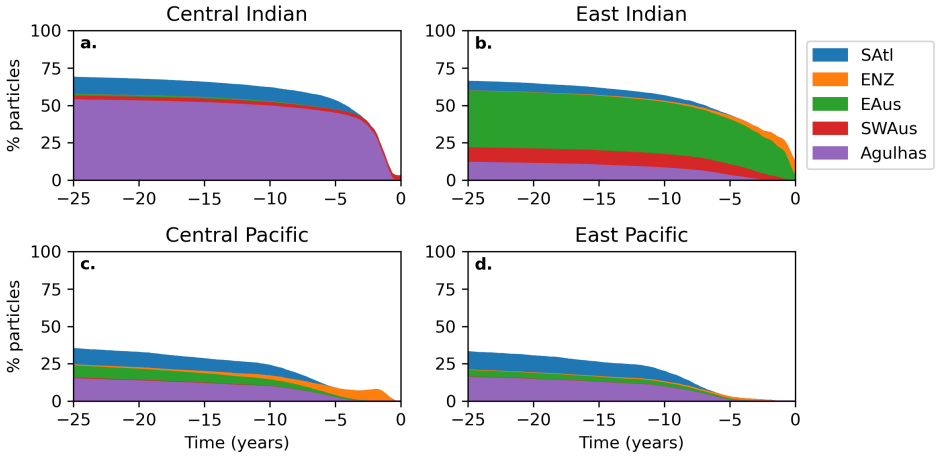

Figure 4. Percentage of particles transiting through, or leaving the model domain within, continental boundary regions as function of backward time for particles originating in the different SAMW formation regions. Boundary regions: South Atlantic (SAtl), East New Zeland (ENZ), East Australia (EAus), Southwest Australia (SWAus), Agulhas Current (Agulhas).

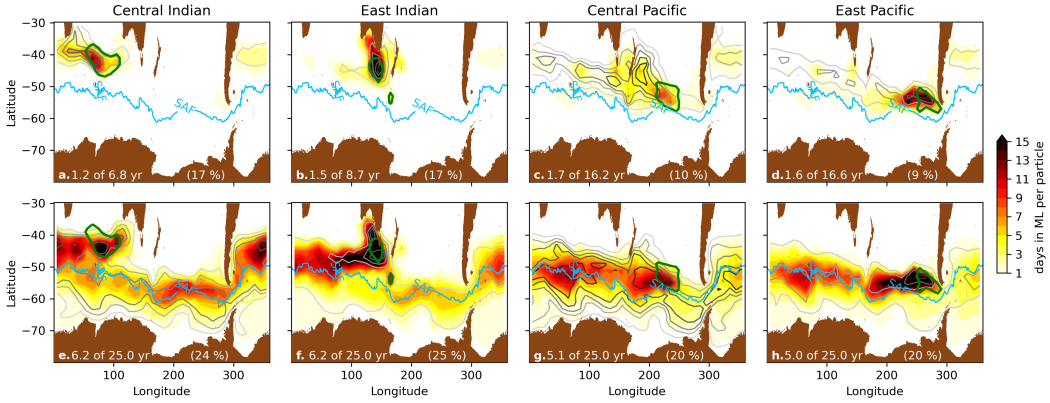

Figure 5. Location and duration of mixed layer exposure: spatial distribution of all particle observations (grey contours) and length of ventilation events (time in mixed layer, ML) (colours) for particles released in the different SAMW formation regions. The upper row (**a-d**) shows is for particles following a northern pathway (end location north of the sub-Antarctic Front), and the lower row (**e-h**) is for particles following a southern pathway (end location south of the sub-Antarctic Front). The distribution of particles at the time of release is shown by a green contour (encircling bins with particle concentrations above 33% the peak concentration). Mean time spent in the mixed layer, mean time from release to leaving the model domain, and % of time spent in the mixed layer are reported for each pathway and formation region. The light blue contour delineates the position of the sub-Antarctic Front (SAF).

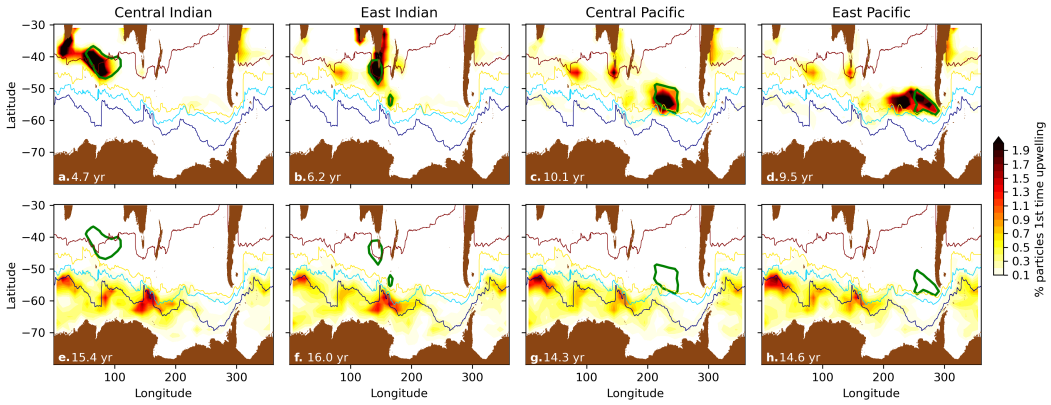

Figure 6. Spatial distribution of locations of first-time particle upwelling into the surface mixed layer. The upper row (**a-d**) shows is for particles following a northern pathway (end location north of the sub-Antarctic Front), and the lower row (**e-h**) is for particles following a southern pathway (end location south of the sub-Antarctic Front). The distribution of particles at the time of release is shown by a green contour (encircling bins with particle concentrations above 33% the peak concentration). Mean time spent between earliest upwelling and SAMW formation is reported for each pathway and formation region. Thin contours delineate the positions of the ACC's fronts; from south to north: ACC Southern Boundary (SB, dark blue), the Polar Front (PF, light blue), the Sub-Antarctic Front (sub-AF, yellow) and the Subtropical Front (STF, red).

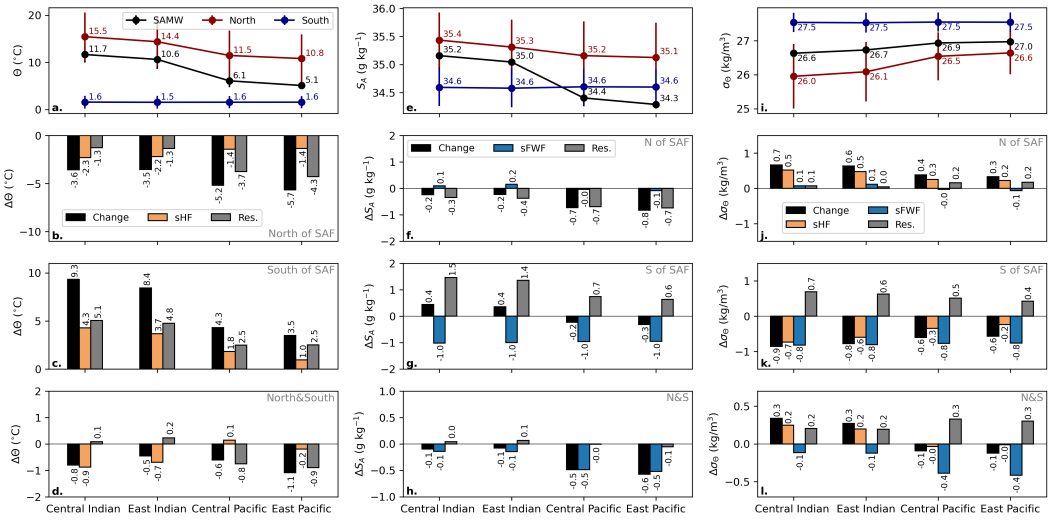

Figure 7. Values and changes in conservative temperature (Θ, **a-d**), absolute salinity (S_A, **e-h**) and potential density (σ_Θ, **i-l**) between their release location at the SAMW mixed layers to their end location (at the end of the simulation or at the time they leave the model domain). Particles are split between those following the northern pathway (end location to the north of the sub-Antarctic Front) and the southern pathway (end location to the south of the sub-Antarctic Front). Panels **a, e, i** show the mean properties of the particles at the release and end location. Panels **b, f, j** and **c, g, k** show the contribution of air-sea fluxes (yellow: heat, blue: freshwater) and ocean mixing (residual, gray), to the net change (black) in properties for the northern and southern pathways, respectively. Panels **d, h, l** show the same mean contributions when all particles, following northern and southern pathways, are considered together.

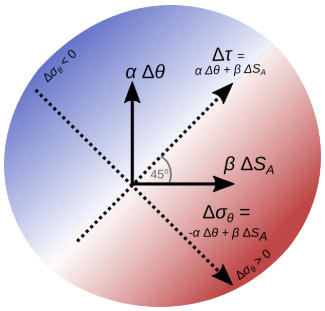

Figure 8. Schematic representation of the meaning of the vectors and colour contours in Figs. 9, S1. The eastward and northward component of the vectors indicate the S_A and Θ changes/fluxes scaled by the β and α factors, respectively, thus representing its contribution to potential density changes ($\Delta\sigma_\theta$). Purely diapycnal transformations occur along the $\Delta\sigma_\Theta = -\alpha\Delta\Theta + \beta\Delta S_A$ axis, with pure densification ($\Delta\sigma_\Theta > 0$) at $-45°$ (red filling) and lightening ($\Delta\sigma_\Theta < 0$) at $+135°$ (blue filling). Purely isopycnal transformations (i.e., changes in spice, τ) occur along the $\Delta\tau = +\alpha\Delta\Theta + \beta\Delta S_A$ axis (white filling). Arrows at 45° indicate a density-compensated warming and salinification, while arrows at -135° indicate a density-compensated cooling and freshening.

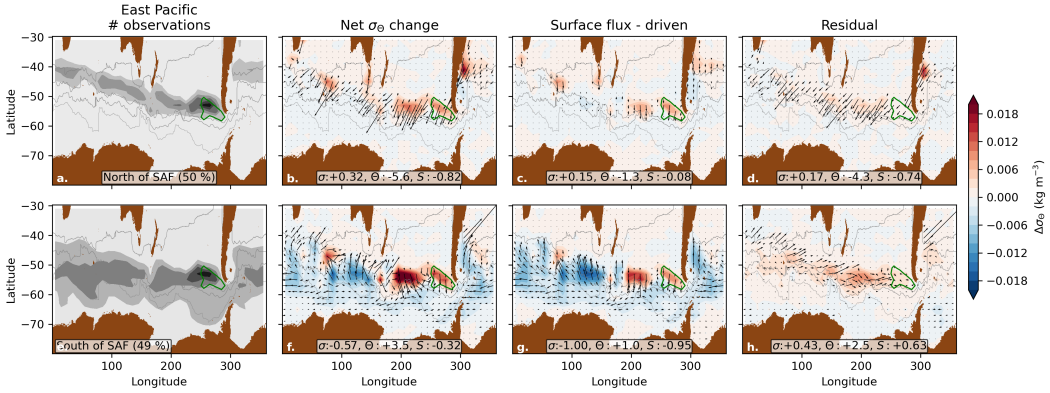

Figure 9. Spatial distribution of the mean changes in potential density (σ_Θ), conservative temperature (Θ) and absolute salinity (S_A) along particle trajectories for particles released at the SAMW formation region in the east Pacific Ocean. Changes in σ_Θ are represented by filled blue-red contours, and changes in S_A and Θ (scaled by their contribution to density changes using the β and α factors) are represented by the magnitude of the arrows in the x and y directions, respectively (Figure 8). The upper row (**a-d**) is for particles following the northern pathway (end location north of the sub-Antarctic Front), and the lower row (**e-h**) is for particles following the southern pathway (end location south of the sub-Antarctic Front). **a, e** show the distribution of particle positions throughout the simulation; **b, f** show the mean net changes, and **c, g** the surface flux contribution to the net changes. Panels **d, h** show the residual between the net and the surface flux-driven changes, which is attributed to mixing. Mean values of the changes and fluxes for all particles and locations are shown in the white boxes. The percentage of particles following the northern and southern pathways are shown in **a, e**. Green contours represent the distributions at release time, encircling bins with particle concentrations above 33% the maximum concentration at time zero.

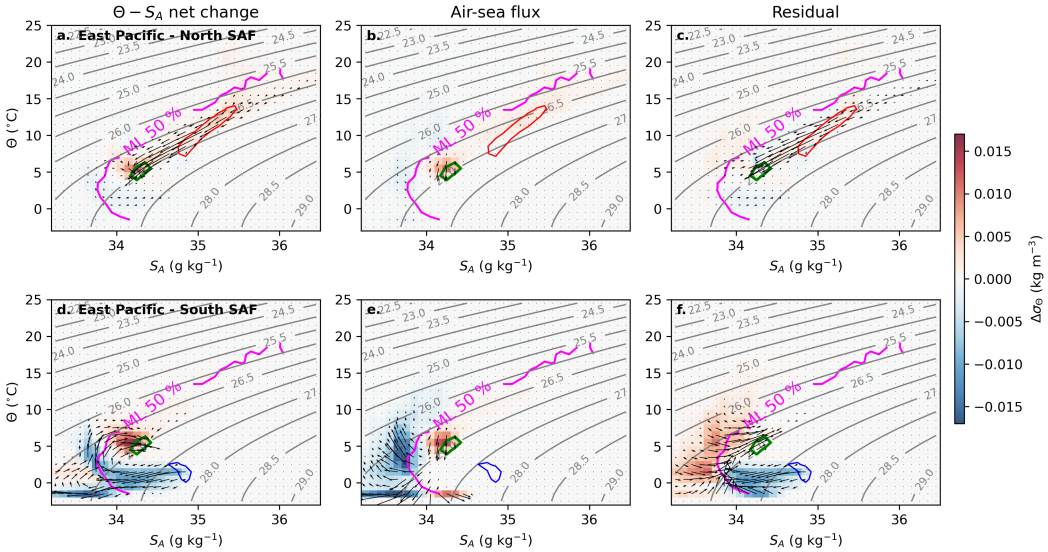

Figure 10. Distribution in the Θ-S_A space of the contribution to mean changes in potential density (σ_Θ), conservative temperature (Θ) and absolute salinity (S_A) along particle trajectories for particles released at the SAMW formation region in the east Pacific Ocean, for the northern (upper row), and southern (lower row) particle pathways. Changes in σ_Θ are represented by filled blue-red contours, and changes in S_A and Θ are represented by the magnitude of the arrows in the x and y directions, respectively. Panels **a, d** show the mean net changes, and **b, e** the surface flux contribution to the net changes. Panels **c, f** show the residual between the net and the surface flux-driven changes, which is attributed to mixing. The magenta line separates Θ-S_A recorded mostly when particles are located at the mixed layer (> 50% instances within the mixed layer, upper left corner) from those recorded mostly when particles are in the ocean interior (< 50% instances within the mixed layer, lower right corner). The distribution of particles at the time of release, depicting SAMW properties, is shown by a green contour. The distribution of particles at the end of the backward simulation, depicting the properties of northern and southern source waters, are shown by a red and blue contour, respectively. Green, blue and red contours encircle bins with particle concentrations above 33% the respective maximum concentration.

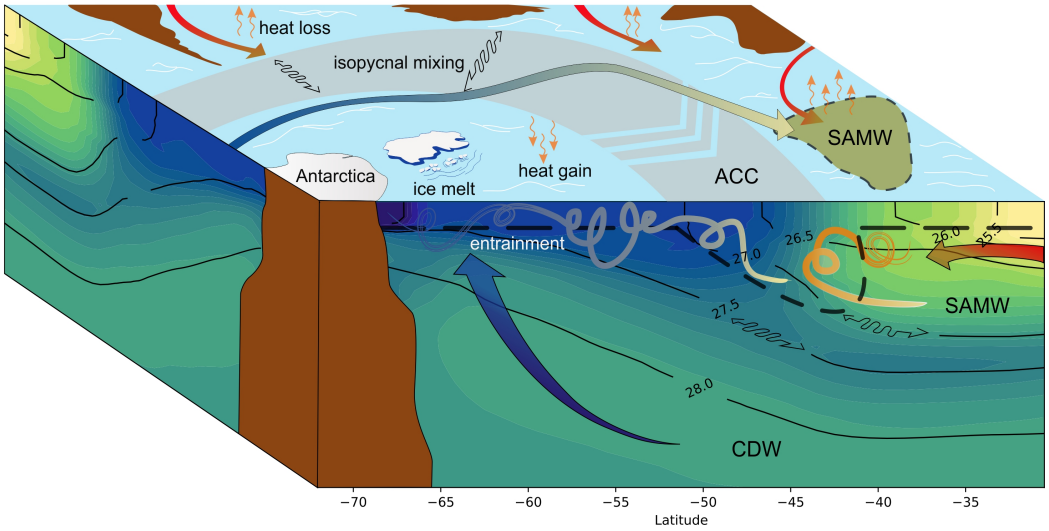

Figure 11. Schematic representation of the two main pathways leading to Sub-Antarctic Mode Water (SAMW) formation: the subtropical pathway of thermocline waters entering the Antarctic Circumpolar Current (ACC) at the western boundaries, and an Antarctic pathway linked to the upwelling of Circumpolar Deep Water (CDW). The arrows and lines, indicating water mass pathways, are filled with colour gradients representing the progressive transformation of warmer/saltier (red) subtropical sources and colder/fresher Antarctic sources (blue) into SAMW, with intermediate properties (yellow). The main processes involved in the transformation of CDW and thermocline waters into SAMW are represented, including: surface heat fluxes, freshwater fluxes due to ice melt, and mixing through entrainment into the mixed layer and isopycnal stirring. The winter mixed layer depth is represented by a thick dashed line. Thick black lines represent lines of equal neutral density. The region of deep mixed layers where SAMW is formed is represented in the horizontal plane by green shading enclosed by black dashed contour. The background contours represent the salinity distribution (low: blue, high: yellow) across a latitude-depth section.